

# Experimental study of polarization properties of highly birefringent photonic crystal fibers

T. Ritari and H. Ludvigsen

Fiber-Optics Group, Department of Electrical and Communications Engineering, Helsinki University of Technology,  
P.O.Box 3500, FI-02015 HUT, Finland  
[Tuomo.Ritari@hut.fi](mailto:Tuomo.Ritari@hut.fi)

M. Wegmuller, M. Legré, and N. Gisin

Group of Applied Physics, University of Geneva, 20 Ecole-de-Medecine, CH-1211 Geneva, Switzerland

J. R. Folkenberg and M. D. Nielsen

Crystal Fibre A/S, Blokken 84, DK-3460 Birkerød, Denmark

**Abstract:** We analyze experimentally the polarization properties of highly nonlinear small-core photonic crystal fibers (PCFs) with no intentional birefringence. The properties of recently emerged polarization maintaining PANDA PCFs are also investigated. The wavelength and temperature dependence of phase and group delay of these fibers are examined in the telecommunications wavelength range. Compared to a standard PANDA fiber, the polarization characteristics and temperature dependence are found to be qualitatively different for both types of fibers.

©2004 Optical Society of America

**OCIS codes:** (230.3990) Microstructure devices; (260.1440) Birefringence; (060.2420) Fibers, polarization-maintaining.

---

## References and links

1. M. D. Nielsen, G. Vienne, J. R. Jensen, and A. Bjarklev, "Modeling birefringence in isolated elliptical core photonic crystal fibers," in *Proceedings of Laser & Electro-Optics Society*, vol. 2, 707-708, San Diego, USA, (2001).
2. J. R. Folkenberg, M. D. Nielsen, N. A. Mortensen, C. Jakobsen, and H. R. Simonsen, "Polarization maintaining large mode area photonic crystal fiber," *Opt. Express* **12**, 956-960 (2004), <http://www.opticsexpress.org/abstract.cfm?URI=OPEX-12-5-956>.
3. T. Ritari, T. Niemi, M. Wegmuller, N. Gisin, J.R. Folkenberg, A. Pettersson, and H. Ludvigsen, "Polarization-mode dispersion of large mode-area photonic crystal fibers," *Opt. Commun.* **226**, 233-239 (2003).
4. J. Noda, K. Okamoto, and Y. Sasaki, "Polarization-maintaining fibers and their applications," *J. Lightwave Technol.* **LT-4**, 1071-1088 (1986).
5. A. Peyrilloux, T. Chartier, A. Hideur, L. Berthelot, G. Mélin, S. Lempereur, D. Pagnoux, and P. Roy, "Theoretical and experimental study of the birefringence of a photonic crystal fiber," *J. Lightwave Tech.* **21**, 536-539, (2002).
6. T. Nasilowski, P. Lesiak, R. Kotynski, M. Antkowiak, A. Fernandez, F. Berghmans, and H. Thienpont, "Birefringent photonic crystal fiber as a multi-parameter sensor," in *Proceedings of Laser & Electro-Optics Society*, 29-32, Enschede, The Netherlands (2003).
7. M. Legré, M. Wegmuller, and N. Gisin, "Investigation of the ratio between phase and group birefringence in optical single-mode fibers," *J. Lightwave Tech.* **21**, 3374-3378 (2003).
8. G. Statkiewicz, T. Martynkien, and W. Urbanczyk, "Measurements of modal birefringence and polarimetric sensitivity of the birefringent holey fiber to hydrostatic pressure and strain," *Opt. Commun.* **241**, 339-348 (2004).
9. A. Michie, J. Canning, K. Lyytikäinen, M. Åslund, and J. Digweed, "Temperature independent highly birefringent photonic crystal fibre," *Opt. Express* **12**, 5160-5165 (2004), <http://www.opticsexpress.org/abstract.cfm?URI=OPEX-12-21-5160>.
10. B. Huttner, J. Reecht, N. Gisin, R. Passy, and J. P. Von der Weid, "Local birefringence measurements in single-mode fibers with coherent frequency-domain reflectometry," *Photon. Technol. Lett.* **10**, 1458-1460 (1998).
11. M. Wegmuller, M. Legré, and N. Gisin, "Distributed beatlength measurement in single-mode fibers with Optical Frequency-Domain Reflectometry," *J. Lightwave Tech.* **20**, 828-835, (2002).

12. B. L. Heffner, "Automated measurement of polarization mode dispersion using Jones matrix eigenanalysis," *Photon. Technol. Lett.* **4**, 1066-1069 (1992).
  13. S. C. Rashleigh, "Measurement of fiber birefringence by wavelength scanning: effect of dispersion," *Opt. Lett.* **8**, 336-338 (1983).
  14. W. K. Burns and R. P. Moeller, "Measurement of polarization mode dispersion in high-birefringence fibers," *Opt. Lett.* **8**, 195-197 (1983).
  15. S. E. Barkou Libori, J. Broeng, E. Knudsen, A. Bjarklev, and H. R. Simonsen, "High-birefringent photonic crystal fiber," in *Proceedings of Optical Fiber Communication Conference*, paper TuM2, Anaheim, USA (2001).
  16. M. Szpulak, T. Martynkien, W. Urbanczyk, J. Wójcik, and W. J. Bock, "Influence of temperature on birefringence and polarization mode dispersion in photonic crystal fibers," in *Proceedings of 4th International Conference on Transparent Optical Networks*, paper WeP10, Warsaw, Poland (2002).
  17. M. Szpulak, T. Martynkien, and W. Urbanczyk, "Effects of hydrostatic pressure on phase and group modal birefringence in microstructured holey fibers," *Appl. Opt.* **43**, 4739-4744 (2004).
  18. A. W. Snyder and J. D. Love, *Optical Waveguide Theory* (Chapman & Hall, New York, 1983), Chap. 17.
- 

## 1. Introduction

Birefringence in photonic crystal fibers (PCFs) usually results from accidental asymmetries in the cladding-hole lattice or from intentional manipulation of the core and/or cladding structure [1, 2]. While it is possible to fabricate a large-mode area PCF with a very low birefringence [3], it is more difficult to obtain low birefringence in small-core PCFs that are often subject to strong form birefringence. Therefore, small-core fibers are better suited for different sensing and polarization maintaining (PM) applications [4]. Due to the small mode area, such fibers are also highly nonlinear. Nonlinear effects can be avoided by employing novel "PANDA PCFs" that provide relatively large-mode field diameters and endlessly single-mode operation [2]. In a PANDA PCF, birefringence is introduced by stress applying elements as in a standard PANDA fiber. This allows for an accurate control of birefringence over long fiber lengths. PANDA-like PCFs find applications for instance in fiber lasers and gyroscopes.

So far, there exist only little experimental data on the birefringence of PCFs [e.g., 1-3,5-9]. Normally, only the phase or group birefringence is reported, but very seldom both [7,8]. In the presence of strong form birefringence (small-core PCFs), the phase and group birefringence can have very different values [7] and therefore it is important to investigate them both. For standard PANDA fibers on the other hand (as well as for other fibers having large stress birefringence), the phase and group birefringence have quite similar values. Consequently, the ratio of phase to group birefringence can indicate whether the birefringence is rather due to form or stress contributions. An interesting case in that sense is the recently emerged large-mode area PANDA PCFs in which the total birefringence is a combination of stress and form induced birefringence. In practical applications, it is also important to consider the sensitivity of the polarization properties to changes in the environment. PCFs made from one material only are expected to be to a large extent insensitive against temperature fluctuations [9]. This is due to the lack of asymmetric stress which builds up in standard fibers with different core and cladding materials (i.e. dopants). PANDA PCFs, on the other hand, are more prone to temperature changes due to the different thermal expansion coefficient of the stress elements.

In this paper, we study in detail the dependence of phase and group delay of four commercial birefringent PCFs on both wavelength and temperature in the 1500-1600 nm wavelength range. The results are further compared with a standard PM fiber.

## 2. Fiber samples

The PCFs investigated have a triangular cladding-hole structure shown in the optical micrograph images of Fig. 1. In the following, the fibers are labeled as PCF2, PCF3, PANDA5, PANDA7 and PANDA9 according to their type and core diameters of 2, 3.5, 4.9, 7 and 9.1  $\mu\text{m}$ , respectively. The first two fibers are nonlinear small-core PCFs with no intentional birefringence, whereas the latter ones are PANDA polarization maintaining PCFs where the birefringence arises from a stress field generated by two boron-doped silica rods

[2]. PANDA5, PANDA7, and PANDA9 have been fabricated from the same preform by varying the outer fiber diameter, so that one can assume that the relative cladding hole asymmetries are similar in all of the fibers. The cladding-hole pitches,  $\Lambda$ , of the fibers are 1.4, 2.3, 3.2, 4.4 and 5.9  $\mu\text{m}$ , respectively, with air hole diameter to pitch ratios  $d/\Lambda$  of 0.6 and 0.4 for PCF2 and PCF3 and 0.48 for PANDA PCFs. The length of the fiber samples was 20 m for PCF2 and 3-6 m for the other fibers. The standard PM fiber was a 3.5 m long PANDA fiber from Fujikura (SM.15-P-8/125-UV/UV400 PANDA).

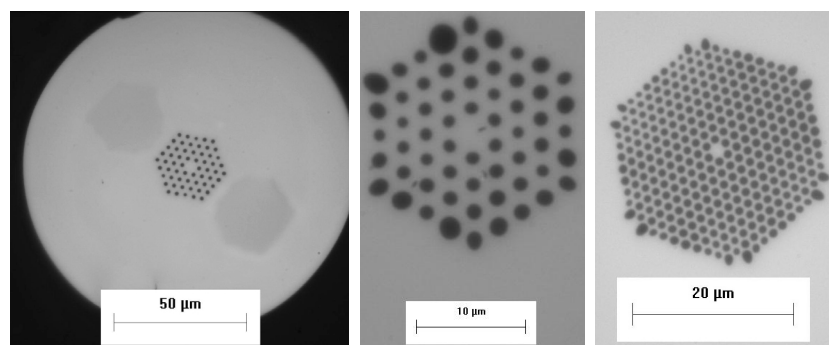


Fig. 1. Cross-sections of the analyzed PCFs. (From left to right) PANDA5 (PANDA7 and PANDA9 have the same cross-section with a different scaling), PCF3, and PCF2.

### 3. Measurement methods for phase and group birefringence

We use the phase delay  $\beta$  and the group delay  $B$  to characterize the corresponding type of birefringence. The phase delay  $\beta$  [s/m] and the phase birefringence  $\beta_{rad}$  [rad/m] can also be expressed in terms of beat length  $L_b$  [m]. The relationship between these widely used terms is represented by the following equation

$$L_b = \frac{\lambda}{c\beta} = \frac{2\pi}{\beta_{rad}}, \quad (1)$$

where  $\lambda$  denotes the wavelength and  $c$  the speed of light. The group delay is on the other hand defined as the frequency derivative of the phase birefringence and is given by

$$B \equiv \left| \frac{\partial \beta_{rad}}{\partial \omega} \right| = \left| \beta - \lambda \frac{\partial \beta}{\partial \lambda} \right|. \quad (2)$$

Therefore, in principle, the measurement of the wavelength dependence of the phase birefringence is sufficient to be able to predict the group birefringence as well. However, the precision of the experimental extraction of  $\beta$  is sometimes (especially for small  $B$ ) insufficient for a precise determination of  $B$ , and we therefore measure both  $\beta$  and  $B$ .

The phase delay  $\beta(\lambda)$  and group delay  $B(\lambda)$  of the fiber samples are investigated using both a polarization-sensitive optical frequency-domain reflectometer (POFDR) [10, 11], and a so-called twist method [7]. The POFDR is a high-resolution coherent reflectometric technique that is used to extract the beat length (phase birefringence) of a fiber but does not yield the corresponding group birefringence. The POFDR measurement gives the beat length at 1550 nm only, whereas the values at other wavelengths can be determined by measuring the corresponding relative change in phase difference using a tunable laser and a polarimeter. This relative phase difference is then added to the known total phase difference at 1550 nm. As the sign of the phase difference is difficult to determine, it was chosen to be equal to the one obtained with the twist method. This latter measurement method uses the standard Jones Matrix Eigenanalysis (JME) -technique [12] to measure  $B(\lambda)$  at different twist rates of the

fiber, and as a result provides both the phase and the group birefringence for the untwisted fiber. Twisting of the fiber induces circular birefringence and mode coupling between the polarization modes: the coupling first leads to a drop in the differential group delay, whereas it starts to increase again for large twist rates where the additional circular birefringence becomes dominant.

#### 4. Wavelength dependence of phase and group birefringence

We measured the birefringence properties of the PCF samples using the POFDR and twist measurement methods described in Section 3. Table 1 shows the corresponding results for a wavelength of 1550 nm. For comparison, Table 1 also shows the measured values of beat length, phase and group delay, and their ratio for a standard PANDA fiber. The latter value of 1.1 agrees well with the previously reported findings for fibers with stress elements [13,14]. In such fibers, both  $\beta$  and  $B$  are essentially constant with wavelength, and have approximately equal magnitude.

Table 1. Birefringence properties of different PCF samples and standard PANDA fiber @ 1550 nm.

	PCF2	PCF3	PANDA5	PANDA7	PANDA9	PANDA
$L_b$ [mm]	8.8 / 8.5	30.7 / 30.7	16.6 / 18.3	14.0 / -	14.4 / -	4.2 / -
POFDR / twist						
$\beta$ [ps/m]	0.597	0.168	0.309	0.369	0.359	1.23
$B$ [ps/m]	0.225	0.213	0.497	0.480	0.392	1.36
$B/\beta$	0.38	1.27	1.61	1.30	1.09	1.1

The values for the beat length obtained with the POFDR and twist methods agree very well for the small-core PCFs (PCF2 and PCF3), whereas the agreement is worse (10%) for PANDA5. The twist method is more difficult to apply on fibers with stress elements, giving somewhat less accurate results. In fact, the beat length of PANDA9 and PANDA7 could not be measured using the twist method due to the mechanical rigidity caused by their larger cladding diameters (230  $\mu\text{m}$  and 175  $\mu\text{m}$ , respectively, compared to 125  $\mu\text{m}$  for PANDA5). Table 1 demonstrates that all PCF fibers are strongly birefringent, although the corresponding phase delays (calculated from the mean beat lengths) are lower than for the standard PANDA fiber. As expected for similar amount of asymmetry, the phase delay  $\beta$  of PCF2 (with a smaller core) is larger compared to the one of PCF3 [15]. The phase delay  $\beta$  of PANDA5, however, is slightly smaller than the one for PANDA9 and PANDA7 despite its smaller core dimension. A possible explanation is that the diameter of the stress elements can vary with the length of the fiber preform [2] and this can cause small birefringence variations from one fiber to another. Another explanation could be that the non-negligible presence of form birefringence in PANDA5 (see below) could lower the total birefringence if its axes are not aligned with those of the stress-induced birefringence.

In order to obtain a group delay at 1550 nm with low measurement noise or statistical fluctuations, we use a second order polynomial fit of  $B(\lambda)$  over a broad wavelength interval around 1550 nm. The corresponding results for  $B$ , given in Table 1, were found to be very reproducible ( $\sim 1\%$  variations) even when the measurements were conducted at different places (Helsinki University of Technology and University of Geneva). Generally, the values seem to be larger for the PANDA PCFs. The  $B/\beta$  ratios are in general quite different from one. Consequently, the birefringence in PCFs seems to be usually influenced by form birefringence. Only for PANDA9 a ratio close to one is found suggesting that form birefringence is negligible [7]. This can be expected since for larger core diameters accidental form birefringence will have a lower impact. This is indeed confirmed by a monotonically decreasing  $B/\beta$  ratio for PANDA5, PANDA7 and PANDA9. Note that even in the presence of form birefringence, a ratio of one can be found at a specific wavelength, and consequently one should measure  $B/\beta$  at different wavelengths in order to be certain that form birefringence is

really absent. This verification is done in the following, and as we will see, form birefringence is indeed found to be negligible in PANDA9, but not in the other PCFs.

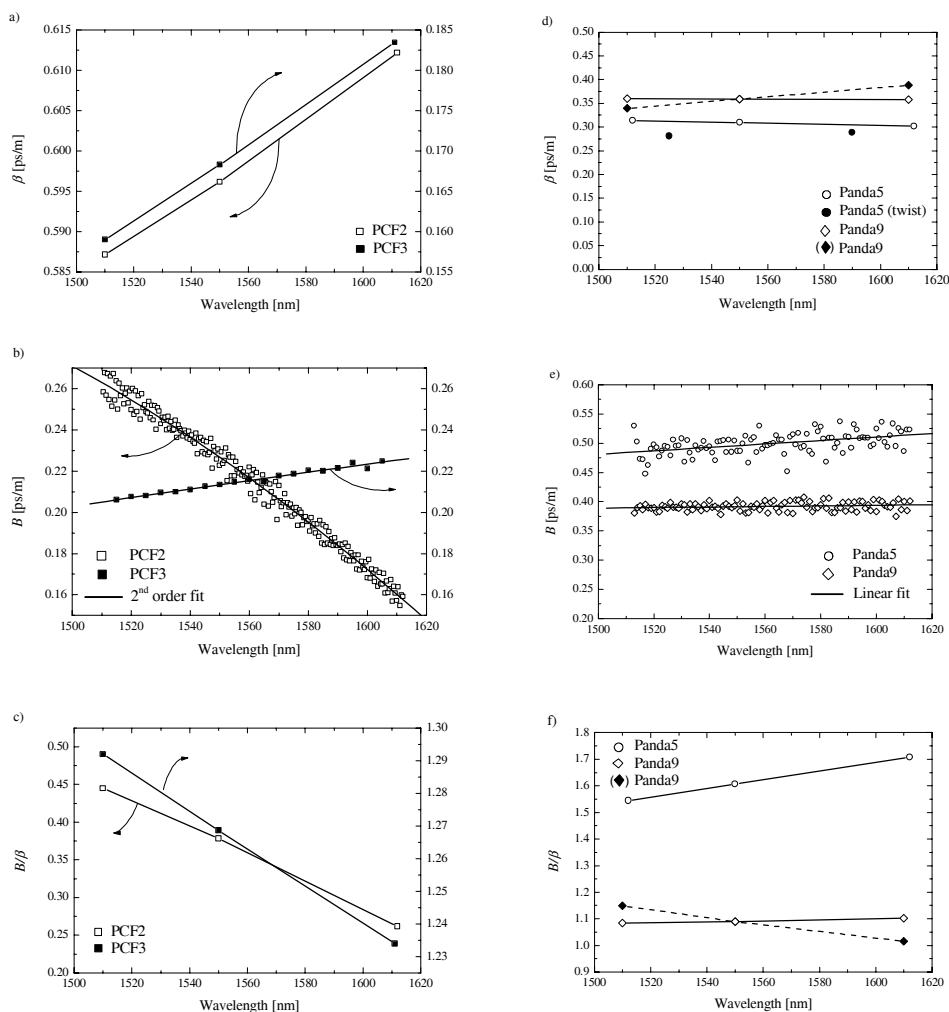


Fig. 2. Phase delay (a,d), group delay (b,e) and ratio of  $B/\beta$  (c,f) as a function of wavelength for PCF2/PCF3 and PANDA5/PANDA9, respectively.

The wavelength dependence of the phase and group delays is shown in Fig. 2. Figure 2(a) shows that for PCF2 and PCF3, phase delay is found to grow almost linearly with wavelength. This is in good agreement with simulations [6,15-17] and also with other similar experiments [5,6,8]. Therefore, it seems that the increase of birefringence with wavelength is a quite general property of a PCF. This behavior can be explained by the fact that the effective core-cladding index difference increases with wavelength resulting in higher birefringence for longer wavelengths, given a constant asymmetry [18].

The phase delay  $\beta(\lambda)$  for the PANDA PCFs is difficult to measure as the twist results, used to determine the sign of the relative phase difference, are either less accurate (PANDA5) or not available (PANDA9 and PANDA7, see beginning of section 4). We focused our study on PANDA5 and PANDA9 which have the smallest and largest core diameters. The phase delay is found to be nearly constant with wavelength for PANDA5 (see Fig. 2(d)). For PANDA9 on

the other hand, depending on the sign of the relative phase change (unknown), the wavelength dependence is either very small (solid curve) or quite large (dashed curve). The first solution looks more reasonable as the  $B/\beta$  ratio (solid curve, Fig. 2(f)) is close to one and almost constant for all wavelengths, strongly suggesting that form birefringence is absent so that one can expect a negligibly small wavelength dependence of both  $\beta$  and  $B$ .

The results for the group delay  $B(\lambda)$  are shown in Figs. 2(b) and 2(e). It is interesting to compare these measured values with the ones calculated from  $\beta(\lambda)$  using Eq. (2). This gives a value of 0.214 ps/m for PCF2 and 0.208 ps/m for PCF3 at 1550 nm. The calculated values agree well with the measured ones of 0.225 ps/m and 0.213 ps/m. A good agreement is also observed for PANDA5 and PANDA9 between the calculated (0.503 ps/m and 0.393 ps/m) and measured values (0.497 ps/m and 0.392 ps/m, respectively). The group delay measurements for PANDA5 and PANDA9 are also in good agreement with the measurements reported in [2] where the group birefringence was measured using the so-called crossed polarizer technique. The wavelength dependence of  $B$  shows that contrary to the behavior of  $\partial\beta/\partial\lambda$ ,  $\partial B/\partial\lambda$  has different size and sign for PCF2 and PCF3 (see Fig. 2(b)). Note that if one ignores the absolute value in Eq. (2) for PCF3, the  $B$  value becomes negative. The meaning of a negative sign is that the fast and slow axes of the phase and the group delay are 'flipped', i.e. the axis with faster phase velocity is at the same time the one with slower group velocity. According to the modeling in [1], a smaller slope of  $B$  is indeed expected for PCF3. For PANDA5,  $B$  is found to slightly increase with wavelength (by a similar amount as in PCF3), whereas for PANDA9,  $B$  is essentially constant with wavelength as expected for a fiber dominated by stress birefringence. In general, the larger the core dimension, the smaller the wavelength dependence of the group delay.

Finally, Figs. 2(c) and 2(f) give the ratio of  $B/\beta$  as a function of wavelength. As expected [7], the ratio changes considerably with wavelength when it is far from one (PCF2, PCF3, and PANDA5), whereas it is fairly constant and close to one for PANDA9. Note that for PANDA5, a high confinement loss was observed in the measurement range. Since the ratio of group to phase delay can be significantly different from one within PCFs, it is important to use the correct type of birefringence at the correct wavelength when predicting the polarization properties of such fibers.

## 5. Temperature dependence of phase and group birefringence

In different sensing and polarization-maintaining applications, it is very important to have a thorough understanding of the temperature sensitivity of the polarization properties. In general, the dependence of the phase birefringence on temperature is characterized by the parameter  $K_T \equiv \partial\beta_{rad}/\partial T$ . We measure this by recording the variation of the output polarization state  $S$  as a function of temperature. In order to do this in a well defined way, the fiber is fixed in a temperature-controlled water bath. One can then easily calculate  $K_T$  from the angular velocity of  $S$  on the Poincaré Sphere, i.e., one period of a given Stokes parameter corresponds to a phase shift of  $2\pi$  in the corresponding temperature interval. This is a relative phase measurement only, and consequently we do not know the sign of  $K_T$ . To go around this problem, we also measured the beat length  $L_b$  as a function of temperature at 1550 nm using the POFDR. From this measurement both the sign and the magnitude of  $K_T$  can be inferred in a straightforward manner. The corresponding results for PANDA PCFs and standard PANDA fiber (see Table 2) are found to agree reasonably well with those obtained from the change of the output polarization. The precision of the POFDR does not however allow to measure changes in beat length below one per cent and therefore no conclusive result about the sign of  $K_T$  for PCF2 could be obtained. It can, however, be reasonably assumed that a change in temperature will change both the phase and group delays in the same manner, and we therefore use the sign found from the measurement of the temperature sensitivity of the group delay reported below.

Table 2 summarizes the results for the temperature dependence of the four fiber samples analyzed. PCF3 was not studied since  $K_T$  is probably small (as for PCF2), and the length of

the fiber would consequently be too short for reasonable measurements. The previously reported change in stress caused by the coating of a PCF [3] was not observed for the present highly birefringent small-core PCFs, and we essentially found the same birefringence values for a fiber piece with and without coating. Indeed, it is expected that the typically encountered external pressures do not have a significant influence on the birefringence of fibers having  $\beta \sim 0.3$  ps/m (corresponds to  $\Delta n \sim 10^{-4}$  [4]). The observed temperature dependence of the birefringence in the fiber samples analyzed here should therefore not depend on their coatings.

Table 2. Temperature sensitivities of phase and group delay @ 1550 nm.

	PCF2	PANDA5	PANDA9	PANDA
$K_T$ [rad/K/m]	0.012 / -	-0.624 / -0.6	-0.601 / -0.6	-2.06 / -1.8
$S_{out}$ / POFDR				
$K_T/\beta_{rad}$ [1/K]	$1.66 \cdot 10^{-5}$	$-1.65 \cdot 10^{-3}$	$-1.38 \cdot 10^{-3}$	$-1.37 \cdot 10^{-3}$
$K_\tau$ [fs/K/m]	0.027	-0.731	-0.564	-1.78
$K/B$ [1/K]	$1.2 \cdot 10^{-4}$	$-1.47 \cdot 10^{-3}$	$-1.44 \cdot 10^{-3}$	$-1.3 \cdot 10^{-3}$

A clear trend is visible for the temperature dependence of the phase delay:  $K_T$  is very small and positive (i.e., the birefringence becomes larger with increasing temperature) for PCF2, whereas a large and negative  $K_T$  is found for the standard PANDA fiber. In PCFs, a temperature change will not introduce stress in the same way as in conventional fibers as there is only one bulk material. Consequently, the influence of temperature on phase delay,  $\beta$ , mainly comes from a change in the effective index difference. The refractive index of the core grows more rapidly with temperature than the effective index of the cladding that is influenced by the more constant index of air. A larger effective index difference then leads to a larger phase delay. This has been verified by modeling two PCF structures with a large form birefringence [16]. The theoretical model has also been backed up by an experiment [6] where a coefficient of  $K_T \sim 0.1$  rad/K/m was found at a wavelength of 633nm. On the other hand, in a standard PANDA fiber, the birefringence induced by the stress-elements strongly decreases with temperature as the initial drawing condition is approached where stress is absent. The same behavior is found in the PANDA PCFs based on the same technology. However, the  $K_T$  values are about three times smaller than for the standard PANDA fiber (see Table 2). A plausible explanation is that part of the stress field acting on the core is 'screened' (i.e., lowered) by the cladding hole structure [2]. Intuitively, the screening grows with the air-filling fraction of the PCF cladding (with no air holes, one has a standard PANDA fiber, whereas for an air-fill fraction of one, the core becomes mechanically detached and therefore experiences no stress). This same effect could also explain the lower phase birefringence  $\beta$  (factor of about four with respect to the standard PANDA fiber, see Table 1). It is also important to investigate the  $K_T$  values normalized with  $\beta$ . They can act as a figure of merit for the temperature dependence of the phase as one can argue that a larger birefringence will typically be more susceptible to temperature changes. Table 2 shows that the normalized phase delay for PCF2 changes about 100 times less with temperature than for the PANDA-like PCF or standard PANDA fibers. This illustrates that highly-birefringent PCFs are valuable candidates for polarimetric pressure sensors [6] or PM-interferometers with better temperature stability.

Interestingly, the normalized  $K_T$  values are almost identical for the three fibers with stress elements. We believe that this can be explained by the fact that the same type of stress elements are used in all these fibers leading to the equal change of stress with temperature. Although the birefringence resulting from this asymmetric stress field differs among the fibers due to a different scaling factor (i.e., due to the above described screening), its relative change with temperature will remain the same.

Figure 3 shows the wavelength dependence of  $K_T$  in the 1500 to 1600 nm wavelength range. Although the measurement was difficult to perform due to the small temperature dependence,  $K_T$  clearly increases with wavelength for PCF2 (the error bars in the figure give the maximum deviation in the results from different measurement series). This behavior

coincides with the model of [16] and the intuitive assumption that a larger  $\beta$  will lead to a larger  $K_T$  as well. The temperature dependence is also found to increase with wavelength for the standard PANDA fiber (however  $K_T$  is negative due to the previously mentioned reasons), whereas the opposite trend is found for the PANDA-like PCFs (absolute value decreases with wavelength). We do not readily have an explanation for this surprising behavior.

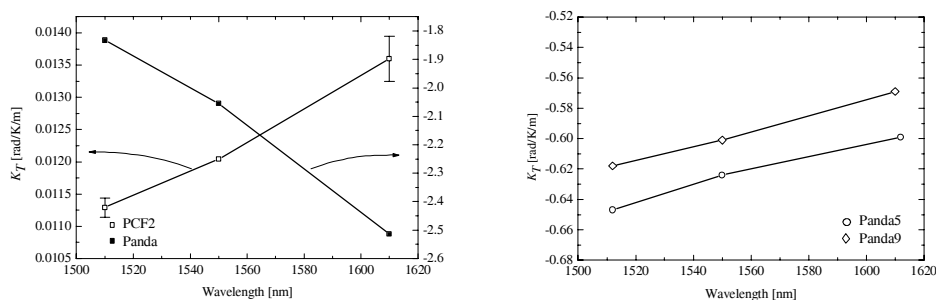


Fig. 3.  $K_T$  as a function of wavelength. Arrows indicate corresponding scales.

The temperature sensitivity of the group delay  $B$  was determined by measuring  $B$  at 1550 nm as a function of temperature using the same temperature-controlled water bath described above. The parameter  $K_T \equiv \partial B / \partial T$  was then obtained from a linear fit to the measurement results. To precisely determine the group delay  $B$ , we used a wavelength interval of at least 10 nm around 1550 nm. The change of  $B$  as a function of temperature was found to be extremely small for PCF2, and therefore it was important to well stabilize the temperature during a JME-scan in order to obtain a good reproducibility of the results. A very small and positive  $K_T$  was found for PCF2 whereas a considerably larger and negative  $K_T$  was found for the PANDA and PANDA-like PCFs (see Fig. 4). In contrast to our measurement for PCF2, a negative  $K_T$  was found from a numerical modeling of a more asymmetric but otherwise similar PCF in [16], indicating that  $K_T$  might critically depend on the exact fiber geometry.

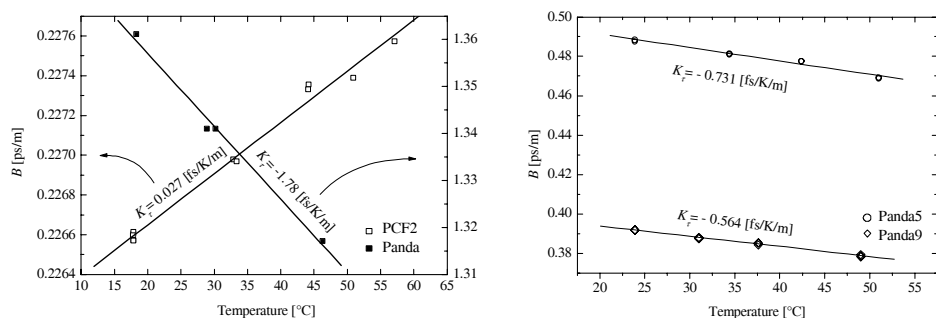


Fig. 4.  $B$  as a function of temperature @ 1550 nm (averaged over at least 10 nm intervals). Arrows indicate corresponding scales.

Comparison of the normalized  $K_T$  values (Table 2) shows that the group delay in PCF2 changes about 10 times less than in the PANDA and PANDA-like PCFs, for which the normalized  $K_T$  values are again very similar. Also, the relative change of the group delay with temperature is about seven times larger than that of the phase delay for PCF2, whereas the two are about equal in the fibers with stress-applying elements.



## 6. Conclusion

We have conducted an experimental analysis of the temperature and wavelength dependence of phase and group delay for different highly birefringent PCFs in the telecom wavelength range. In three of the PCFs, the birefringence was based on stress-applying elements. The results have been compared with a standard PANDA fiber.

We found that the phase delay  $\beta$  increases nearly linearly with wavelength in two small-core PCFs. This is in agreement with other experimental results and numerical modeling and it therefore seems to be a general property of a PCF. However, the wavelength dependence of the group delay  $B$  is different for the above mentioned PCFs. For the PCF with the smaller core,  $B$  decreases with wavelength whereas for the larger core fiber it increases with wavelength. Consequently, the ratio of the group to phase delay is found to depend on the dimensions and the exact geometry of the fiber. In addition, the ratio is highly wavelength dependent and can have a considerably different value from one. For the PANDA-like PCFs, where the birefringence is largely induced by stress-applying elements, the birefringence and its wavelength dependence are found to depend on the core dimension. The larger core PANDA PCF has similar polarization properties as a standard PANDA fiber while the smaller core fibers are subject to some amount of form birefringence as well and, consequently, their properties are somewhere between small-core PCFs and standard PANDA fibers. Therefore, it is very important to perform a detailed polarization analysis for both the small-core and PANDA-like PCFs.

Finally, compared to the PANDA-like PCFs and the standard PANDA fiber, the relative temperature sensitivities of the phase and group birefringence for a small-core PCF were found to be smaller by a factor of 100 and 10, respectively. This shows that small-core PCFs are valuable candidates to relax temperature stability constraints in polarization maintaining applications whereas large-core PANDA-like PCFs could prove to be useful in high-power applications where single-mode operation is essential.

## Acknowledgments

The work at Helsinki University of Technology has been financially supported by the Academy of Finland and the graduate school of Modern Optics and Photonics. Part of this work was conducted during a Short Term Scientific Mission within the European COST P11 project. GAP at Geneva University acknowledges financial support from the Swiss OFES (COST P11) and EXFO Electro-Optical Engineering Inc., Québec.